Reverse Engineering : Investigation on the Material Trends in Lithium-ion Battery

HORIBA

We obtained lithium-ion battery cells from 3 different commercial electric vehicles manufactured by an automotive company for the reverse engineering investigation. We named the samples "Model A," "Model B," and "Model C" here. Model A is the newest and Model C is the oldest vehicle model among the three samples. We disassembled and analyzed each of the cathode sheets, the anode sheets, and the separator sheets using multiple analytical instruments.

Director and organizer : Nikkei BP,
Collaborative partners :Yamagata University, Osaka Research Institute of Industrial Science and Technology, The Japan Steel Works, Ltd., HORIBA Techno Service Co., Ltd.

(Example)	Entire cell	Cathode sheet	Anode sheet	Separator sheet
Model A sample		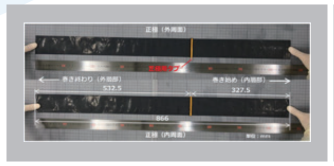	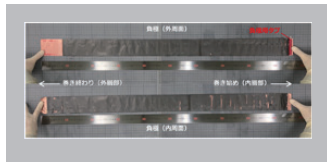	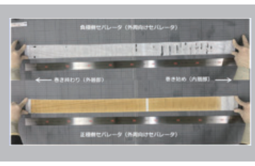

Photo courtesy of the above disassembled lithium-ion battery cells: ATTACCATO LLC.

Result Summary

The material trends used in different lithium ion battery cells

- **Cathode** : All the cathode samples contained Ni and Co, but the newer model showed higher Ni/Co ratio.
- **Anode** : The oldest model used only carbon materials, but the newer anodes contained Si material, as well.
- **Separator** : All the separator sheet had alumina coating and polyamide coating on the base polymer materials.

More detailed information can be referred in Nikkei BP website https://project.nikkeibp.co.jp/bpi/#anchor_report

Cathode

We determined **elemental compositions of the cathode sheets** from the 3 battery cell samples using the HORIBA MESA-50 X-ray Fluorescence Analyzer. Focusing on Ni content, our result showed that the cathode sheet from the Model A sample contained the highest Ni content, followed in order by the Model B sample, and the Model C sample. It indicates that cathode materials varied depending on the manufacturing timing, and we could see a trend toward higher-nickel material in their cathode sheet samples.

Table C1. The nickel content comparison among the cathode sheets from the 3 different battery cell samples.

Element	Model A (the newest vehicle model)		Model B		Model C (the oldest vehicle model)	
	wt	mol %	wt	mol %	wt	mol %
Ni	92.532	91.07	88.835	87.69	88.735	81.8

We performed **elemental mapping on the cathode sheets** from the 3 battery cell samples using the HORIBA XGT-9000 X-ray Analytical Microscope. Figure C1 shows a result of elemental mapping on the Figure C1 shows a result of elemental mapping on the cathode sheet from the Model A sample. The result shows that Co and Ni are uniformly distributed in the cathode sheet. Unexpectedly, Fe and Al were detected on the peeling part of the cathode layer, where a cathode current collector is exposed.

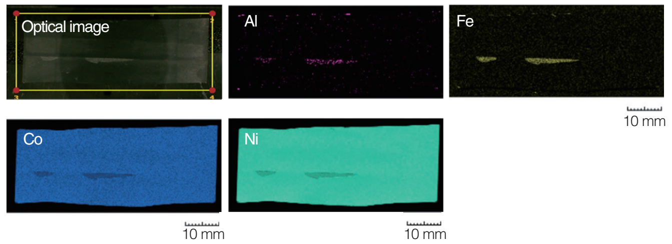

Figure C1. Elemental mapping result of the cathode sheet from the Model A sample (the newest model) using the HORIBA XGT 9000.

We carried out **elemental depth profile analysis on the cathode sheets** from the 3 battery cell samples using the HORIBA GD-Profiler 2 Glow Discharge Optical Emission Spectrometer. Figure C2 shows the elemental depth profiles starting from cathode surface to cathode current collector. Based on the result, we could see the trend that the cathode sheet from the newer model had a higher Ni/Co ratio, and the result was consistent with the trend found in the Table C1. In addition, Fe was detected, as well as Al around 6000 sec, in each profile. The result suggested that these cathode current collectors are not pure aluminum but aluminum alloy containing iron.

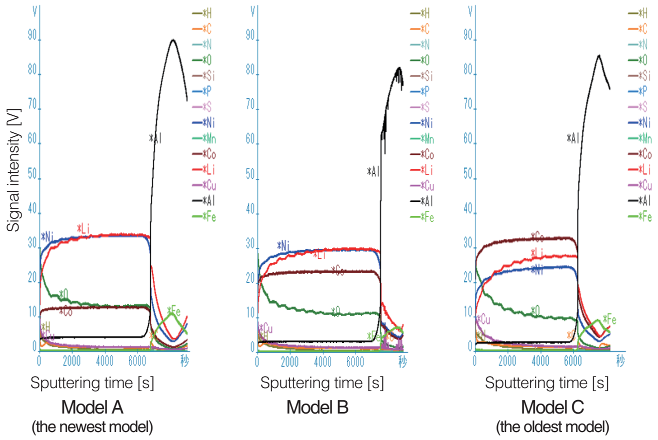

Figure C2. Elemental depth profiles of the cathode sheets from the 3 different battery cell samples using the HORIBA GD Profiler 2.

We performed **chemical composition analysis on the cathode sheets** from the 3 battery cell samples using HORIBA LabRAM HR Evolution Confocal Raman Microscope. Figure C3 shows chemical composition imaging results processed based on classical least square model. The results show that the cathode sheets from different cell samples had different mixing ratios of an active material, a conductive additive, and a binder material. We could see the trend that a cathode sheet from the newer model had less active material.

(Red: active material, Green : conductive additives and binder)

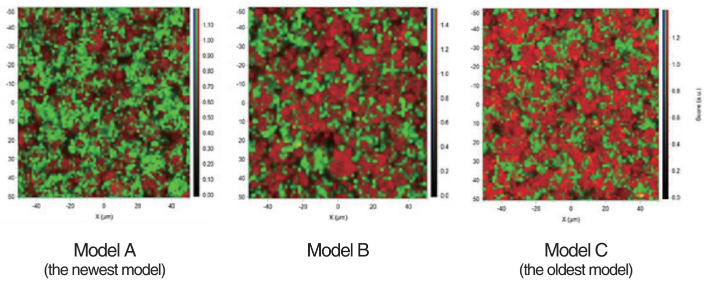

Figure C3. Chemical composition imaging results of the cathode sheets from the 3 different cell samples using the HORIBA LabRAM HR Evolution.

Anode

We conducted **surface observation and elemental mapping on the anode sheets** from the 3 different samples using a SEM-EDX. Figure A1 shows a SEM image and elemental images of the anode sheet from the Model A sample. Based on Figure A1, two different particles seemed to exist in the anode sheet. The elemental map results showed not only carbon (C) but also oxygen (O) and silicon (Si) in the anode sheet. The O image and the Si image both had the same distribution. It suggests that the anode sheet contained silicon oxide, as well as carbon material.

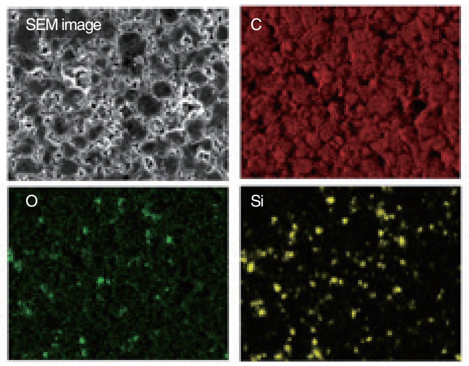

Figure A1. SEM image and elemental images of the anode sheet from the Model A sample (the newest model) using a SEM-EDX.

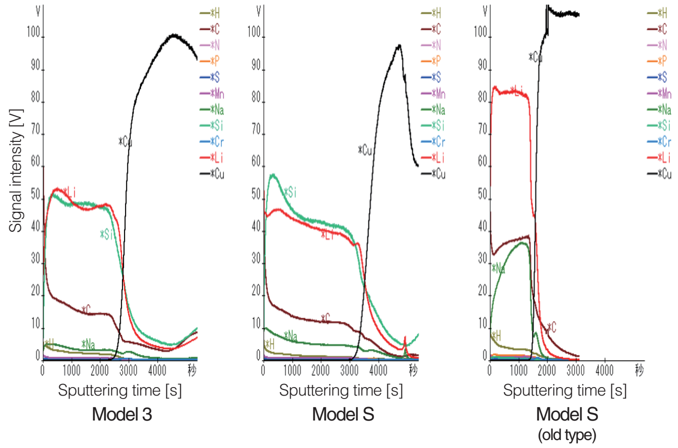

We carried out **elemental depth profile analysis on the anode sheets** from the 3 different samples using the HORIBA GD-Profiler 2 Glow Discharge Optical Emission Spectrometer. Figure A2 shows the elemental depth profiles starting from anode surface to anode current collector. The depth profile results show that Si was detected in the anode sheets from the 2 newer model samples (Model A and Model B), while Si was not detected in the oldest model sample (Model C).

Figure A2. Elemental depth profiles of the anode sheets from the 3 different samples using the HORIBA GD-Profiler 2.

We performed **chemical composition imaging on the anode sheets** from the 3 different samples using the HORIBA LabRAM HR Evolution Confocal Raman Microscope. Figure A3 shows chemical imaging results processed based on the classical least square model. The results show that the anode sheets from the Model A sample and the Model B sample contained silicon particles, in addition to carbon materials such as graphite and amorphous carbon particles. This result was consistent with our result shown in Figure A2.

(Green : graphite, Red : amorphous carbon, Pink : high crystalline silicon, Blue : silicon, Light blue : low crystalline graphite)

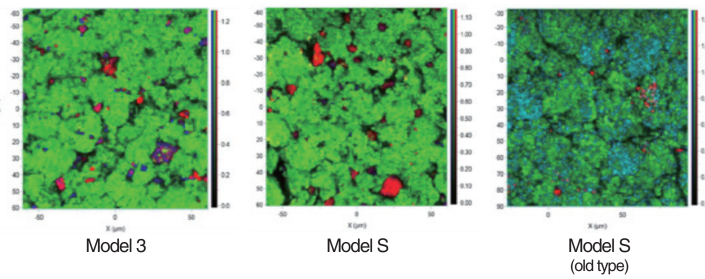

Figure A3. Chemical composition imaging results of the anode sheets from the 3 different samples using the HORIBA LabRAM HR Evolution.

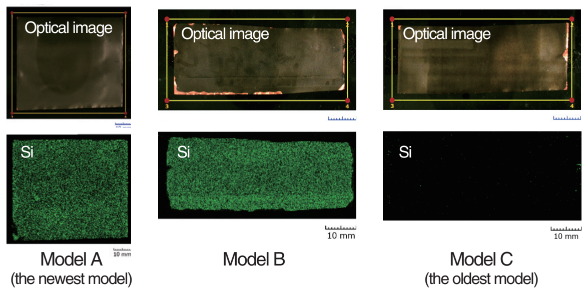

We performed **elemental mapping on the anode sheets** from the 3 different samples using the HORIBA XGT-9000 X-ray Analytical Microscope. The results show that Si was detected in the anode sheets from the 2 newer model samples (Model A and Model B), while Si was not detected in the anode from the oldest model (Model C). It is consistent with our previous results in Figure A2 and A3.

Figure A4. Elemental mapping result of the anode sheets from the 3 different samples using the HORIBA XGT-9000.

Separator

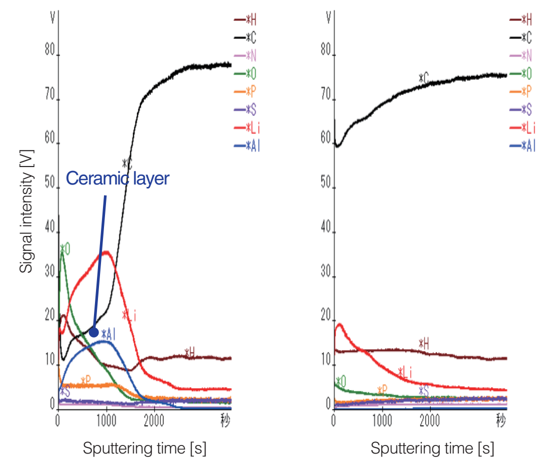

Model A (sputtering from the surface in cathode side)

Model A (sputtering from the surface in anode side)

We carried out **elemental depth profile analysis on the separator sheet** from the Model A sample using the HORIBA GD-Profiler 2 Glow Discharge Optical Emission Spectrometer. Figure S1 (a) shows the elemental depth profile starting from the separator surface on the cathode side, and Figure S1 (b) shows the profiles starting from the separator surface on the anode side. Compared with the two profiles, we found Al in the second layer only on the cathode side.

Figure S1. Elemental depth profiles of the separator sheet from the Model A sample using the HORIBA GD-Profiler 2.
(a) profile starting from the surface in cathode side.
(b) profile starting from the surface in anode-side.

We performed **chemical composition analysis on the separator sheets** from the 3 different samples using the HORIBA LabRAM HR Evolution Confocal Raman Microscope. Figure S2(a) shows Raman spectrum results of each separator surface on the cathode side. Figure 2(b) shows the spectrum matching with a reference spectrum of poly(p-phenylene terephthalamide), a kind of aromatic polyamide. It suggested that the polyamide material is used on the top surface coating on the separator.

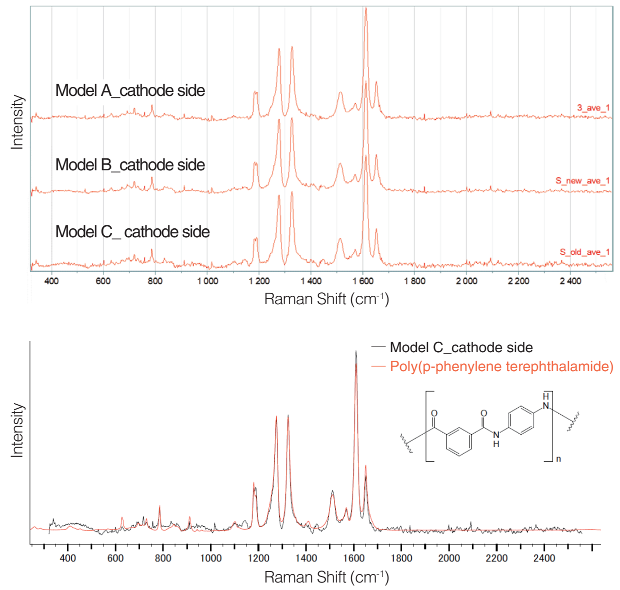

Figure S2. (a) Raman spectrum results of each separator surface in the cathode side using the HORIBA LabRAM HR Evolution. (b) Spectrum matching result between the Model C sample (the oldest model) and the reference spectrum of poly(p-phenylene terephthalamide).

X-ray Fluorescence Analyzer

MESA-50

- Fast and non-destructive elemental analysis
- Detectable element range: Al – U
- Spot size: 1.2 mm, 3 mm, 7 mm
- LN2-free detector and pump-free optics design

X-ray Analytical Microscope

XGT-9000

- Fast and non-destructive elemental imaging
- Flexible analysis environment (XGT-9000 Pro): whole vacuum, helium purged (Optional), partial vacuum, air
- Mapping size: 100 mm x 100 mm

Multimodal Confocal Raman Microscope

LabRAM Soleil

*Successor model of LabRAM HR Evolution for lithium-ion battery material analysis.

- Non invasive chemical composition analysis
- Ultra-fast confocal imaging with SmartSampling and Swift patented technologies
- Dedicated software analysis module for lithium-ion battery carbon-based materials

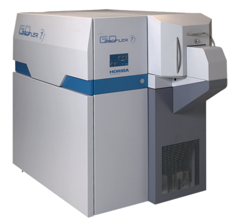

Glow Discharge Optical Emission Spectrometer

GD-Profiler2

- Fast and multiple-element depth profile including lithium.
- RF source in pulsed mode for damage-less analysis with higher depth resolution
- Li Bell, a vessel for air-sensitive samples

Electrified vehicle evaluation solutions

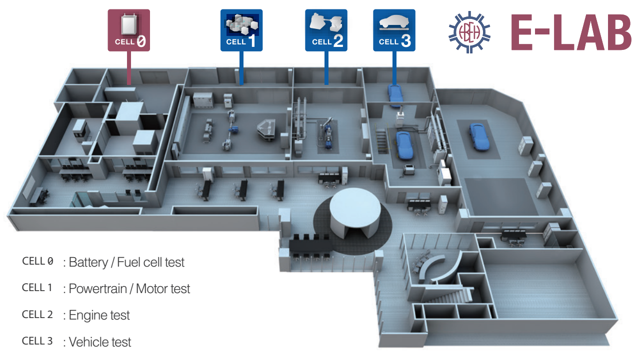

At its automotive measurement R&D/production base, HORIBA BIWAKO E-HARBOR in Shiga Prefecture, HORIBA has a test center, E-LAB,where visitors can "see," "use," and "experience" the effects of automotive measurement solutions.
E-LAB will introduce "Test in the Loop™", HORIBA's proposed solution to improve system calibration efficiency, using actual test equipment.
HORIBA proposes "Test in the Loop™*," which enables the evaluation of components and vehicle systems in a simulated the real-driving environment by freely connecting fuel cell, battery, motor, powertrain, engine, vehicle or its model and evaluation devices. This enables highly accurate performance verification and system optimization of components and systems in the vehicle development and design phases.

* Test in the Loop" is a registered trademark or trademark of HORIBA, Ltd.

Battery and electric vehicle development solutions

HORIBA provides a wide range of development support solutions, from evaluation of on-board batteries themselves and vehicle evaluation based on the simulation of actual use of on-board batteries through to battery model development, optimization design, prototyping, and evaluation.

Model development / prototyping

Battery module/pack development support

HORIBA MIRA provides support for the development of efficient, high energy density battery modules and packs according to customers' requests.

Determining requirements We hear your requests and determine the requirements of the battery pack to be prototyped.

Battery module/pack design

BMS development and design

Designing a more efficient and optimal battery management system (BMS)

- Modeling and simulation analysis of the battery system
- BMS software design and optimization
- Verification by hardware-in-the-loop simulation (HILS)

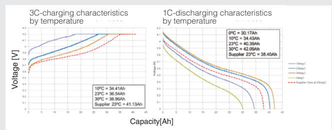

Thermal management system design

Developing and designing of integrated thermal management

- Heat load, battery cooling/heating performance
- Analysis of electric power characteristics in the battery drive cycle
- Synthetic analysis of cooling and air conditioning equipment

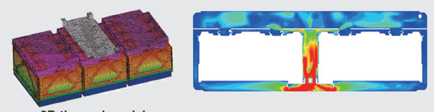

3D thermal model

We also carry out various designing services, including architecture design and battery pack structure design.

Prototyping and evaluation

Using advanced engineering skills to create a prototype according to the requirements and design

- Joining of cells/modules
- Assembly of electrical harnesses and temperature sensors
- Assembly of power electronics devices (fuses, connectors)
- Assembly of water cooling/air cooling units, etc.

Design Optimization

Evaluation method that contributes to electrified vehicles power train optimization: Test in the Loop™

By simulating the vehicle environment using Test in the Loop™, battery performance such as battery charging and discharging characteristics and thermal management can be evaluated in an environment incorporated into the vehicle system.You can evaluate the charging and discharging behavior of an actual battery under the condition in which it is connected to the powertrain while a running road load is imposed upon it as well as evaluate battery performance by changing the ambient temperature.

* Test in the Loop is a registered trademark or trademark of HORIBA, Ltd.

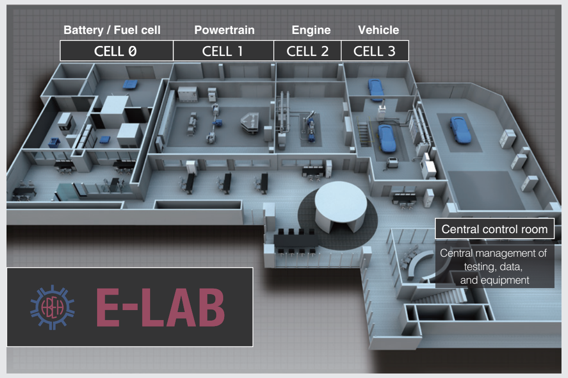

The E-LAB automobile measurement and test center where HORIBA's advanced solutions can be seen, used, and experienced.

Test-piece: Battery
Test equipment: Battery test station, thermostatic chamber

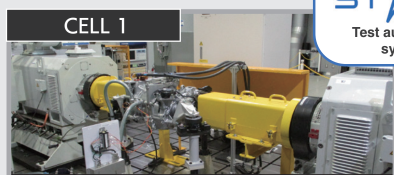

Test-piece: Motor
Test equipment: Dynamometer, general-purpose inverter

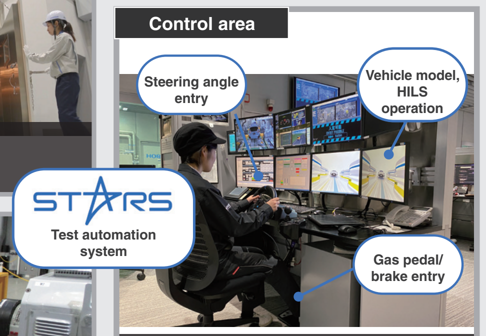

Test equipment: Test automation system, vehicle simulator

Evaluation

Charging and discharging characteristics evaluation

Features

- Support for a power range of up to 1 MW
- Electrical efficiency: 95% or above
- Response speed (t90): Less than 3 ms

The charging and discharging characteristics of driving batteries and stationary storage batteries can be evaluated.We have a lineup of battery test stations that support everything from driving cells, modules, and packs to large stationary storage batteries.

Automotive | Housing | Factory | Power system

Battery test station

Evaluator B